ELSEVIER

Polymer 41 (2000) 2781–2793

polymer

Crystallization and melting behavior of regioregular poly(3-dodecylthiophene)

S.L. Liu[a,b], T.S. Chung[a,b,*]

[a]*Institute of Materials Research and Engineering, 10 Kent Ridge Crescent, Singapore, Singapore 119260*
[b]*Department of Chemical and Environmental Engineering, National University of Singapore, 10 Kent Ridge Crescent, Singapore, Singapore 119260*

Received 11 January 1999; received in revised form 7 June 1999; accepted 1 July 1999

Abstract

Non-isothermal and isothermal crystallization and melting behavior of regioregular poly(3-dodecylthiophene) (P3DT) was investigated by differential scanning calorimetry (DSC) with an emphasis on the main chain crystallization. P3DT showed a sharp exothermic peak at 114°C which was attributed to the main chain crystallization and a broad one peaked at 59°C which was due to the side chain crystallization during cooling at 2.5°C/min from the isotropic melt. During heating, the side chains melting took place from 27 to 80°C, while the main chains melting consisted up to three overlapped melting peaks. Avrami analysis for the non-isothermal crystallization revealed two linear regions with a sharp transition in the $\log(-\ln(1-\theta))$ vs. $\log t$ plots at the relative crystallinity of 63% for all cooling rates studied. The average Avrami exponent, n, was around 4.9 when the relative crystallinity was lower than 63%, while the n was around 1.5 when the relative crystallinity was higher than 63%. The Ozawa method failed to describe the non-isothermal crystallization process. The non-isothermal crystallization activation energy was estimated to be 222 kJ/mol by the Kissinger method, which was in good agreement with that of isothermal crystallization. Isothermal crystallization and subsequent melting were also investigated at different temperatures. The formations of ordered structures were highly dependent on the crystallization temperatures and time. At lower crystallization temperatures, three melting peaks could be discerned. However, only one melting peak could be observed when the crystallization temperature was high.

Keywords: Crystallization; Melting; Regioregular poly(3-dodecylthiophene)

1. Introduction

Conducting polymers, such as polyacetylene, polypyrrole, polythiophene, etc. have attracted much attention because of their potential applications in light emitting diodes, non-linear optical materials, and electrochromic devices [1]. But in general, these conjugated polymers are difficult to dissolve in organic solvents, which limits their processability and applications. The introduction of a side chain to the backbone would greatly enhance their solubility and processability [2]. Based on this idea, many 3-position substituted polythiophenes with various substituents have been reported [3–7]. Among which poly(3-alkylthiophene)s (P3ATs) with various side chain lengths (C_nH_{2n+1}) ranging from 4 to 18 exhibited good solubility and fusibility, and have been extensively studied [8–10].

Poly(3-dodecylthiophene) (P3DT) with 12 carbon atoms in the side chain exhibited good electric conductivity, thermochromism and solubility [11]. Tashiro et al. [12] studied the crystal structure of P3DT by WAXD, and the orthogonal unit cell in P3DT crystals was determined at room temperature to be: $a = 25.83$ Å, $b = 7.75$ Å, $c = 7.77$ Å. P3DT exhibited layered structure. The length of the c-axis obtained by energy calculations for the fully extended planar polythiophene chain was in good agreement with X-ray fiber diffraction results, two planar thiophene rings in the opposite directions. The length of the a-axis calculated from XRD experiments suggested that the alkyl chains are directed along the a-axis. The effective length of the fully extended all-*trans* alkyl chain is about 23 Å in the lateral direction where the van der Waals radii of the atoms are taken into consideration [13], manifesting that the side chains mainly take *trans*-conformation.

Early studies on P3ATs paid little attention to the regularities of the molecular configurations [12,14]. As a result many conflicting results were obtained. Some groups [12]

* Corresponding author. Department of Chemical and Environmental Engineering, National University of Singapore, Singapore. Tel.: +65-874-6645; fax: +65-779-1936.
E-mail address: chencts@nus.edu.sg (T.S. Chung).

0032-3861/00/$ - see front matter
PII: S0032-3861(99)00490-5

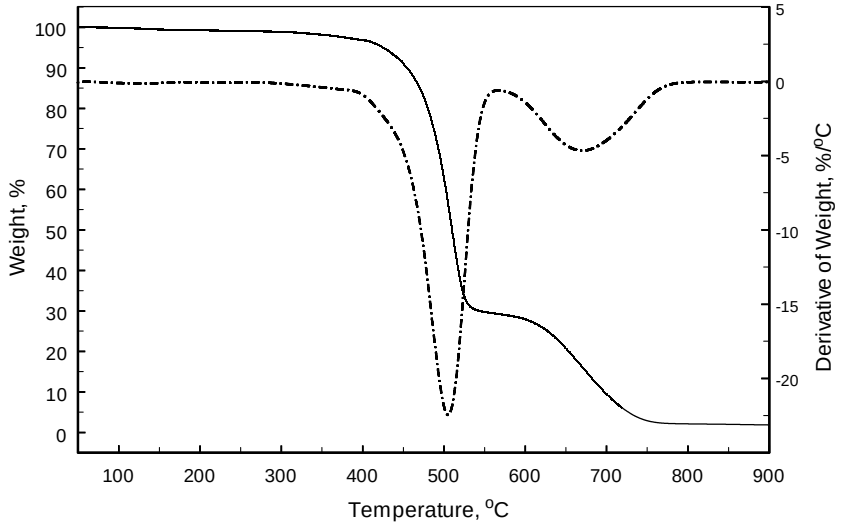

Fig. 1. Weight loss of P3DT in air at 10°C/min.

indicted the existence of isosbectic point during heating, referring that the polymers possess a two-phase morphology; while others observed a continuous blue shift upon heating. There are three possible couplings in poly(3-alkylthiophene)s: head-to-tail diad (HT), head-to-head diad (HH) and tail-to-tail diad (TT). Different synthesis methods would result in P3ATs with different HT diad content. Samples obtained by nickel catalyzed dehalogenation polycondensation of 3-hexyl-2,5-diiodothiophene yields P3ATs with >90% HT diad content; while P3ATs synthesized by chemical oxidation of 3-alkylthiophenes with $FeCl_3$ have a ~80% HT diad content [15]. Investigation revealed that the thermochromic behavior in P3ATs was controlled by the head-to-tail diad content and the side chain length. P3ATs with moderate HT diad content generate a clear thermochromic isosbectic point irrespective of the side chain length [16]. On the contrary, regioregular P3ATs with a diad content >90% exhibited either a continuous blue shift or an isosbectic point. The different thermochromic characteristics are attributed to the subtle morphological differences between the polymers. P3ATs with moderate HT regularity are formally amorphous with a quasi-ordered phase dispersed in the continuous disordered phase. P3ATs with high HT regularity consist of crystalline, quasi-ordered and disordered phases.

The order–disorder transition in P3DT was studied by DSC and optical microscopy [17]. The formation of the ordered structure was highly affected by the crystallization temperature. The double melting character was explained to be associated with the formations of a well ordered phase with a lower melting temperature and a less ordered phase with a higher melting temperature. However, this seems to be contrary to the fact that the melting temperatures of crystalline phase are proportional to their crystal sizes and degree of crystallinity in general.

Despite the fact that large amount of information on the crystal structure and chromatography properties was available, few studies could be found for the kinetics analysis of regioregular P3DT. It is the purpose of this investigation to understand the crystallization and subsequent melting behavior and ordering process during crystallization of regioregular P3DT. The isothermal and non-isothermal crystallization experiments were performed, and the kinetics analysis results are analyzed.

2. Experimental

2.1. Material

The regioregular poly(3-dodecylthiophene) (P3DT) used in this study was purchased from Sigma–Aldrich Chemical. Co. The regioregularity of this P3DT is greater than 98.5% according to the supplier. The chemical structure of P3DT is shown below. The sample was dried at 100°C under vacuum for 24 h prior to use.

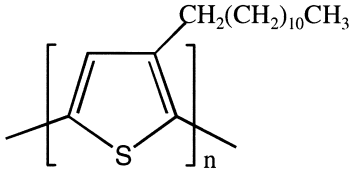

Chart 1. Chemical structure of P3DT

The thermal stability of P3DT was determined by a Perkin–Elmer thermogravimetric analyzer TGA-7. The weight loss of P3DT in air environment with a heating rate of 10°C/min is shown in Fig. 1. The typical two-step weight loss processes were observed. In general, the first

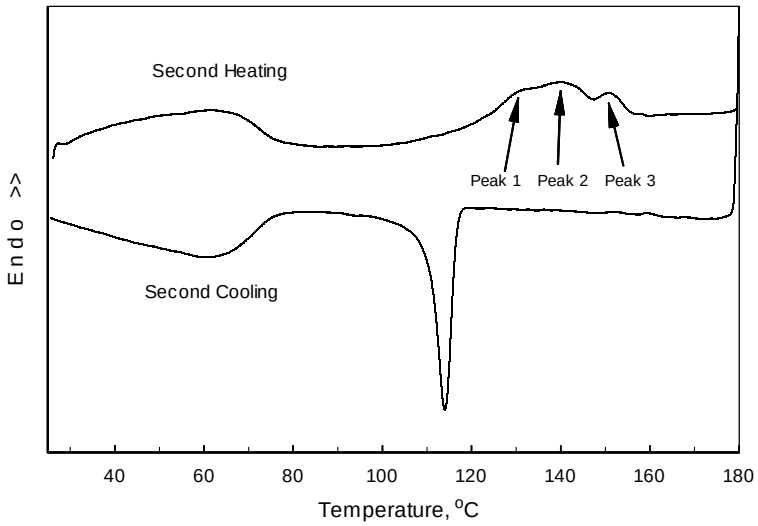

Fig. 2. DSC heating and cooling curves for P3DT at 2.5°C/min.

weight loss was resulted from the random chain scission and carbonization, and the second step was due to the combustion. For thermal analysis experiment in this study, the maximum temperature employed was 200°C to avoid any possible thermal decomposition.

2.2. DSC experiments

All crystallization characterizations of P3DT was performed by using a Perkin–Elmer Pyris-1 differential scanning calorimetry (DSC). The temperature range chosen in this work was from 25 to 200°C. The instrument was calibrated with high purity indium and zinc. The normally used heating rate was 20°C/min. All the experiments were conducted in sealed pans under dry nitrogen environment with a flow rate of 20 psi. For isothermal crystallization experiments, all the samples were heated to 180°C and kept for 2 min, then cooled at 40°C/min to the pre-determined isothermal crystallization temperatures (T_c). The heat flow during isothermal crystallization was recorded, or the samples were subsequently heated to 200°C after a period of crystallization time. For non-isothermal study, the cooling and heating rates were 2.5, 5, 10, 15, 20, 25 and 40°C/min.

3. Results and discussion

3.1. Non-isothermal crystallization

3.1.1. Non-isothermal crystallization analysis by Avrami equation

Fig. 2 shows the DSC second heating and cooling curves of P3DT between 25 and 180°C at a rate of 2.5°C/min. During the heating process, a broad peak from 27 to 80°C and another one from 104 to 155°C are found. In fact, the

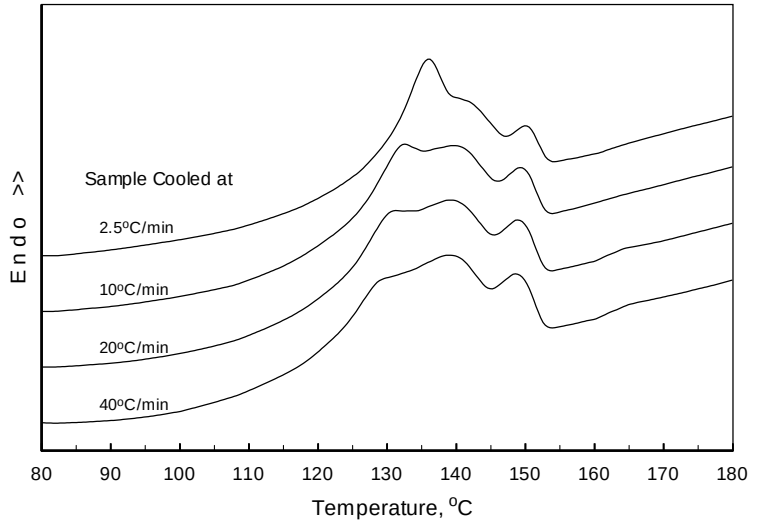

Fig. 3. Set of subsequent heating curves for P3DT cooled at different cooling rates.

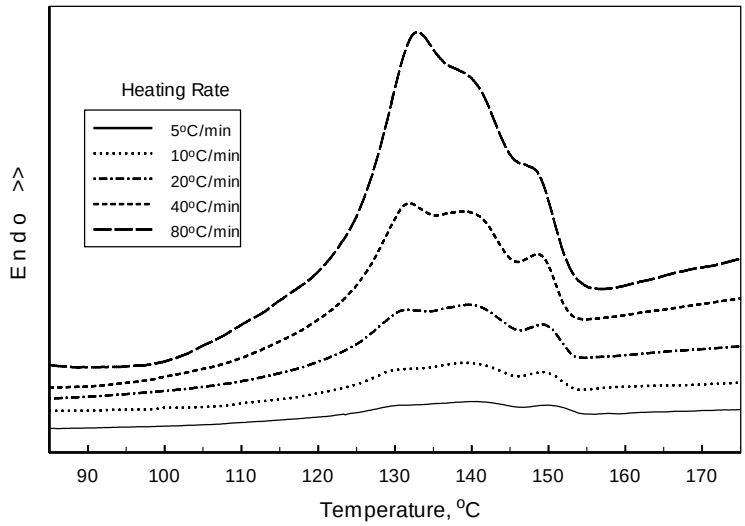

Fig. 4. Set of DSC heating curves with different heating rates.

second melting process consists of three transitions peaked at 130, 139 and 148°C, respectively. During cooling, a sharp exothermic peak at 114°C is found and then a broad exothermic peak from 75 to 25°C. The transition at low temperature during cooling can be described as the side chain crystallization due to high regioregularity and the long chain feature which contains 12 carbons. The side chain crystallization has been reported by Park et al. [17], and it can be better understood as an ordering process. Tashiro's XRD experiments clearly showed that the *h*00 reflections shifted slightly to lower angles and the peaks became more intense and sharper when the temperature was increasing from 35 to 85°C [12]. The sharpening of the diffraction peaks when P3DT was heated from 70 to 80°C is consistent with our DSC experiments that the first endothermic process finishes when it was heated to ~72°C.

XRD results have revealed the layered structure in poly(3-alkylthiophene)s. The length of side chain greatly influences the main chain packing along the *a*-axis. The length of the *a*-axis is almost proportional to the number of carbon atoms of the side chain [18]. In this study we would focus on the main chain crystallization.

In Fig. 3 the DSC subsequent heating curves for the samples cooled from 200°C at different cooling rates are shown. Three distinguishable transitions exist in the sample. It seems that the first transition is more strongly affected by the cooling conditions, which shifts from 130 to 136°C and its relative intensity increases when the cooling rate is decreased from 40 to 2.5°C/min. The second and the third transitions are almost unchanged in their positions and amplitudes with different cooling rates.

The effect of heating rate on the melting behavior of P3DT (all samples have the same thermal history by cooling from 200°C at 40°C/min to room temperature) is shown in Fig. 4. For P3DT samples heated with different heating rates, the first transition moves towards high temperature

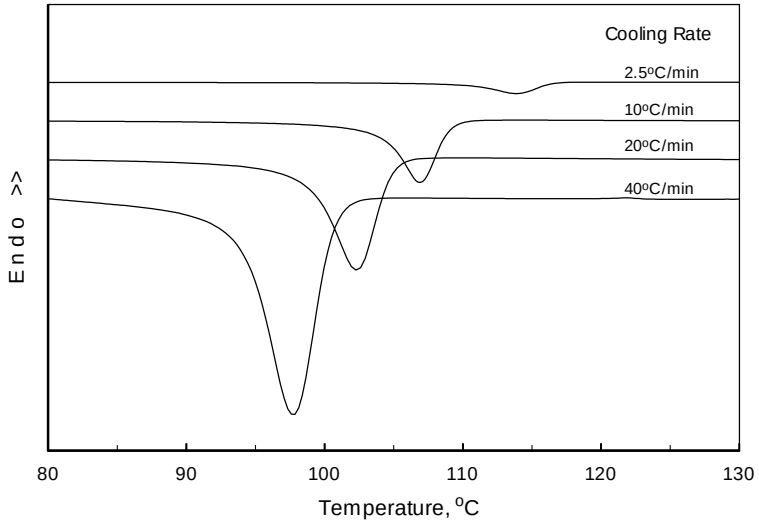

Fig. 5. Set of cooling curves with different cooling rates.

Table 1
Summary of non-isothermal crystallization results

Φ (°C/min)	2.5	5	10	20	25
T_p (°C)	114.05	110.50	106.94	102.28	101.02
ΔH (J/g)	5.432	6.273	7.225	7.746	7.862
θ (T_p) (%)	39.5	36.0	35.8	37.2	38.5

gradually with heating rate. The second one remains unchanged and the third one shifts towards low temperature by 2°C when the heating rate is increased from 2.5°C/min to 40°C/min. It is noted that even with a high heating rate the three melting peaks are still discernible, suggesting that they belong to different melting processes which will be explained below, rather than the melting, reorganization, re-melting process [19].

The effect of cooling rate on the main chain crystallization is shown in Fig. 5. It clearly shows that the cooling rate plays an important role. The exothermic peak shifts from 114°C to 98°C when the cooling rate is increased from 2.5 to 40°C/min. The relative crystallinity achieved at the temperature of maximum crystallization rate, T_p, is not so high as shown in Table 1. The side chain crystallization seems not to be affected by the cooling rate, which further confirms that the crystallization at low temperature is due to the side chains.

For non-isothermal crystallization, the relative crystallinity θ, which is a function of crystallization temperature, can be defined as

$$\theta = \frac{\int_{T_0}^{T} \left(\frac{dH_c}{dT}\right) dT}{\int_{T_0}^{T_\infty} \left(\frac{dH_c}{dT}\right) dT} \quad (1)$$

where T_0 and T_∞ are the initial and end crystallization temperatures, respectively.

The change of relative crystallinity with time is dispalyed in Fig. 6 by converting temperature, T, into time, t, by using Eq. (2)

$$t = \frac{T - T_0}{\Phi} \quad (2)$$

where Φ is the cooling rate.

The Avrami equation can be used for the non-isothermal crystallization analysis as shown in Eq. (3) [20,21]

$$1 - \theta = \exp(-Kt^n) \quad (3)$$

where n is the Avrami exponent, which depends on nucleation and crystal growth; and K is the temperature-dependent constant.

From Eq. (3), the well known double logarithmic plot of $\log(-\ln(1-\theta))$ vs. $\log t$ can be obtained and is shown in Fig. 7. The n and K values are summarized in Table 2. For all the cooling rates studied, all the plots exhibit two linear regions with a transition when the relative crystallinity, θ, is about 63%. When the relative crystallinity is less than 63%, the average of n is about 4.9, suggesting that the primary crystallization for non-isothermal crystallization might be a three-dimensional spherulitic growth with thermal nucleation, while the n in the second linear region is about 1.5. The linear portions in each region are parallel to each other, suggesting the nucleation mechanism and crystal growth are similar for the cooling crystallization process. In polymer melt crystallization, the impingement of spherulites and the secondary or tertiary crystallization will cause the deviation in the double logarithmic plot. This phenomenon was also observed in the non-isothermal crystallization of Nylon-11 [22] and PEEKK [23].

3.1.2. Non-isothermal crystallization analysis by Ozawa equation

Non-isothermal crystallization during cooling is a cooling rate dependent process, which can also be analyzed by the

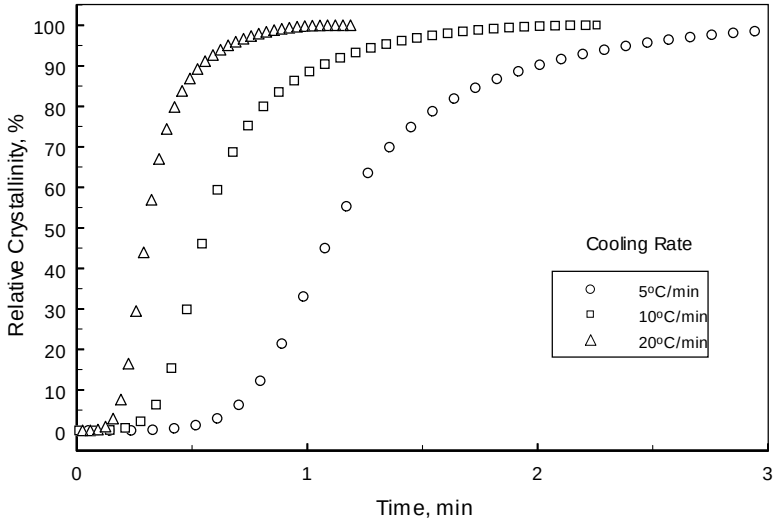

Fig. 6. Plot of relative crystallinity vs. crystallization time.

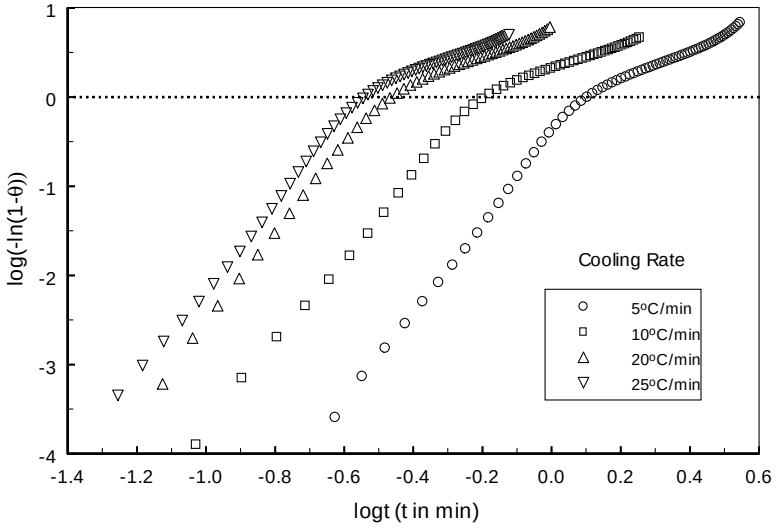

Fig. 7. Plot of $\log(-\ln(1-\theta))$ vs. $\log t$ for non-isothermal crystallization.

Ozawa method [24]. This method accounts for the effect of cooling rate, Φ, on crystallization from the melt by replacing t in Eq. (3) with T/Φ as follows:

$$1-\theta=\exp\left(-\frac{Z(T)}{\Phi^m}\right) \tag{4}$$

where $Z(T)$ is a cooling function of the process, and m is the Ozawa exponent. The value of m is dependent on the dimension of the crystal growth. For three-dimension crystal growth and homogeneous nucleation, m is equal to five. If the Ozawa treatment can correctly describe the non-isothermal crystallization process, a series of straight lines in the $\log(-\ln(1-\theta))$ vs. $\log t$ plot should be obtained, and the Ozawa exponent m can be determined. However, in the case of P3DT non-isothermal crystallization, distinct curvatures in the double logrithmic plots exsist in all the tempertures as shown in Fig. 8, indicting that m is not a constant with temperature. Cebe et al. [25] studied the non-isothermal crystallization of poly(ether ether ketone), and reported the failure of application of the Ozawa method to PEEK non-isothermal crystallzaition. The main reason for the curvatures of the double logarithem curves in PEEK crystallization is attributed to the secondary crystallization. The relative crystallinity values chosen from a given temperature may include values selected from primary crystallization process at one rate and secondary process at another. The curvature makes it impossible for the determination of $Z(T)$ and m. Also the Ozawa method could not properly describe the non-isothermal crystallization of PEEKK [23], liquid crystalline polymer [26] and PEES [27].

Table 2
Kinetics parameters of non-isothermal crystallization

Φ (°C/min)	First linear region		Second linear region	
	n_1	K_1	n_2	K_2
5.0	5.04	0.398	1.69	0.713
10.0	4.71	10.328	1.35	2.086
20.0	4.96	248.313	1.51	5.723
25.0	4.89	493.173	1.50	7.499

3.1.3. The combination of Avrami and Ozawa equation

Ozawa equation cannot describe the non-isothermal crystallization of P3DT owing to different crystallization mechanisms in the cooling process. The crystallinity acheived during cooling is highly associated with cooling rate, Φ, and crystallization time, t. The relation can be established by combining the Avrami Eq. (3) and Ozawa Eq. (4) together [28]:

$$\log K + n\log t = \log Z(T) - m\log\Phi$$
$$\text{or} \qquad \log\Phi = \log F(T) - a\log t \tag{5}$$

where parameter $F(T)=[Z(T)/K]^{1/m}$ refers to the value of cooling rate, which has to be chosen at unit crystallization time when the measured system amounts to a certain degree of crystallinity. a is the ratio of Avrami exponent n to the Ozawa exponent m. Fig. 9 gives a series of parallel lines in the $\log\Phi$ vs. $\log t$ plot at different relative crystallinity. The a and $F(T)$ values are summarized in Table 3. The a values obtained from the P3DT non-isothermal crystallization is quite similar to that from the non-isothermal crystallization of Nylon-11 [22].

3.1.4. Non-isothermal crystallization activation energy

The non-isothermal crystallization activation energy can be derived by the combination of cooling rate and exothermic peak temperature (T_p) shown as Kissinger method

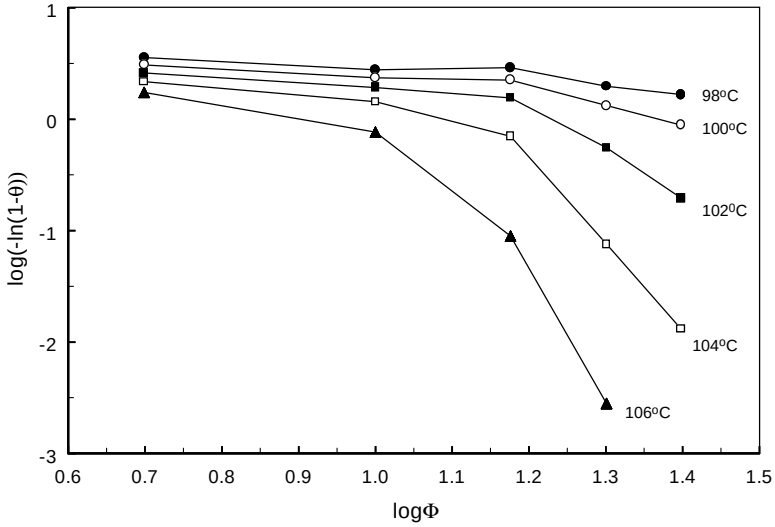

Fig. 8. Ozawa treatment for non-isothermal crystallization of P3DT.

[29] in Eq. (6)

$$\frac{d(\ln(\Phi/T_p^2))}{d(1/T_p)} = -\frac{\Delta E}{R} \quad (6)$$

where R is the gas constant. From the slope of $\log(\Phi/T_p^2)$ vs. $1/T_p$ plot, the non-isothermal crystallization activation energy can be calculated from: $-2.303R \times$ slope. The activation energy is found to be 222 kJ/mol from Fig. 10.

3.2. Isothermal crystallization

The isothermal crystallization analysis is performed at temperatures slightly higher than the onset crystallization temperature during cooling. P3DT can crystallize over a wide range of temperatures, but the relative crystallinity achieved at maximum crystallization rate is not so high, generally less than 40% (Table 4). Therefore, a large portion of crystallinity is achieved in the later stage. Fig. 11 shows the crystallization exotherms of P3DT at different temperatures. From these curves we can see that the major exothermic processes finish within 10 min. The isothermal Avrami treatment for P3DT crystallization is shown in Fig. 12 and Table 4. The Avrami exponent, *n*, is in the range of 2.8–3.8, depending on the crystallization temperature. The crystallization rate parameter *K* decreases with crystallization temperature, T_c.

3.2.1. Isothermal crystallization activation energy

As the polymer crystallization is thermally activated, the

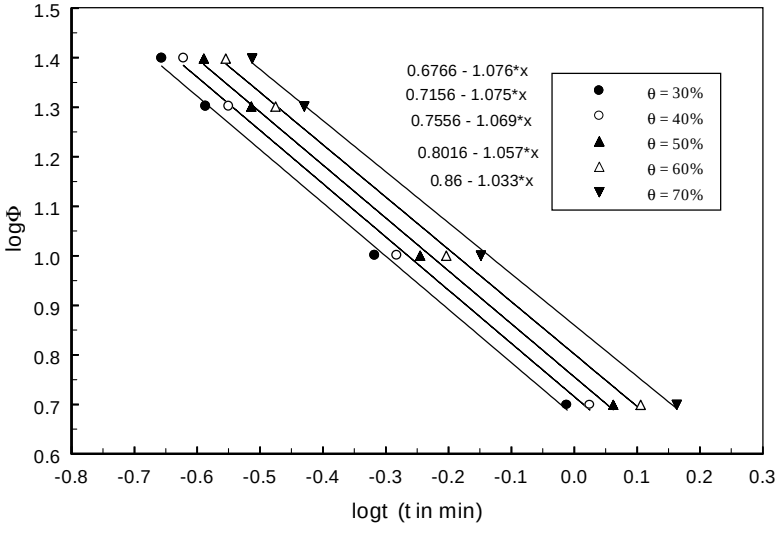

Fig. 9. Plot of log Φ vs. log *t* for the non-isothermal crystallization of P3DT.

Table 3
Kinetics parameters for the non-isothermal crystallization of P3DT by the combination of the Avrami and Ozawa equations

θ (%)	30	40	50	60	70
$F(T)$	0.68	0.72	0.76	0.80	0.86
a	1.08	1.08	1.07	1.06	1.03

crystallization rate K can be described by Arrhenius Eq. (7) [29]:

$$K^{1/n} = K_0 \exp(-\Delta E/\mathrm{R}T_c) \quad \text{or}$$
$$\frac{1}{n} \ln K = \ln K_0 - \frac{\Delta E}{\mathrm{R}T_c} \tag{7}$$

where K_0 is a temperature independent preexponential factor, R the gas constant, and ΔE the crystallization activation energy. ΔE can be determined from the $(1/n)\ln K$ vs. $1/T_c$ plot, which is shown in Fig. 13. The value of the isothermal crystallization activation energy is about 260 kJ/mol. Compared with the non-isothermal crystallization activation energy calculated above, they exhibit good agreement.

3.3. Melting behavior

Tashiro et al. [12] indicated the existence of liquid-crystal (LC) like behavior in P3DT at elevated temperatures. However, optical microscopic studies did not reveal the existence of LC texture in the P3DT samples [19], although LC phases have been observed in some other P3ATs [30]. The subsequent heating experiments for the P3DT samples crystallized at different temperatures for 30 min display an interesting melting behavior as shown in Fig. 14. At lower crystallization temperatures, three melting peaks are found in the heating curves. Their relative amplitudes change with crystallization temperatures. With the increase of crystallization temperature, the first peak increases its amplitude and moves to high temperature. The second and the third peak remain at their positions, but decrease their amplitudes with crystallization temperature. Eventually, the second and the third peak will disappear when the crystallization temperature reaches 119°C. Shown in Fig. 15 are the subsequent heating curves for P3DT isothermally crystallized at 120°C for different times. P3DT samples crystallized less than 2 min exhibit no melting peaks. With the increase of crystallization time, the area of the endothermic peak gradually increases. The isothermal crystallization result at 120°C confirms that only one transition exists. Interestingly, the peak temperature first goes down a little bit with crystallization time, later slightly goes up. It seems that the peak temperature starts to increase when the system has passed the maximum crystallization rate (t_{max}), which is about 6 min as shown in Table 4. It is also noted that the melting peak becomes broader when the crystallization time is prolonged. Generally, the melting peak temperatures should increase with time during isothermal crystallization as the perfection and growth in size of crystals. A discussion regarding this unusual melting behavior will be given later when all the subsequent melting experiments are described.

Park et al. reported the development of endothermic peak at 120°C that the melting peak could only be observed when the crystallization time was longer than half an hour. It

Table 4
Kinetics parameters of isothermal crystallization

T_c (°C)	106	109	112	115	118	120
n	2.8	3.0	2.9	3.0	3.2	3.1
K	8.752	2.570	0.566	0.0605	0.0017	0.0001
t_{max} (min)	0.367	0.583	0.950	1.933	4.383	6.254
$t_{1/2}$ (min)	0.399	0.639	1.097	2.209	4.774	6.832
$\tau_{1/2}$[a] $(\mathrm{min})^{-1}$	2.506	1.565	0.916	0.453	0.209	0.151
θ (t_{max}) (%)	33.94	34.22	29.10	30.11	31.57	30.56

[a] $\tau_{1/2} = 1/t_{1/2}$.

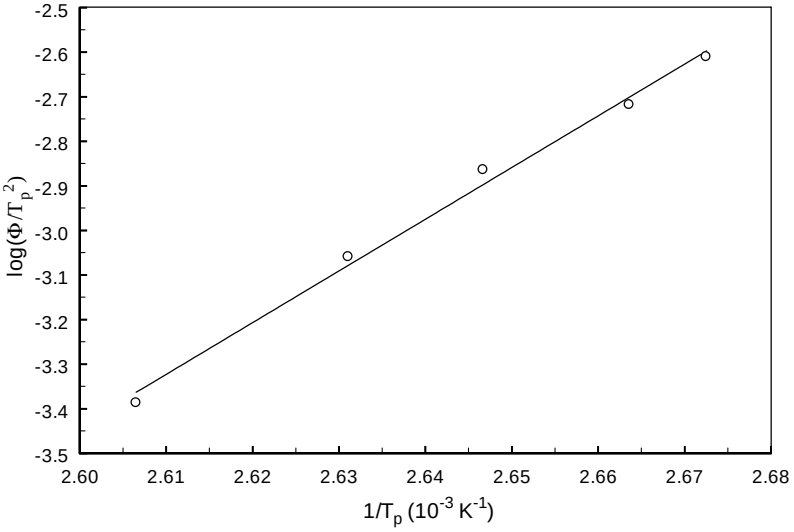

Fig. 10. Kissinger plot for the estimation of non-isothermal crystallization activation energy of P3DT.

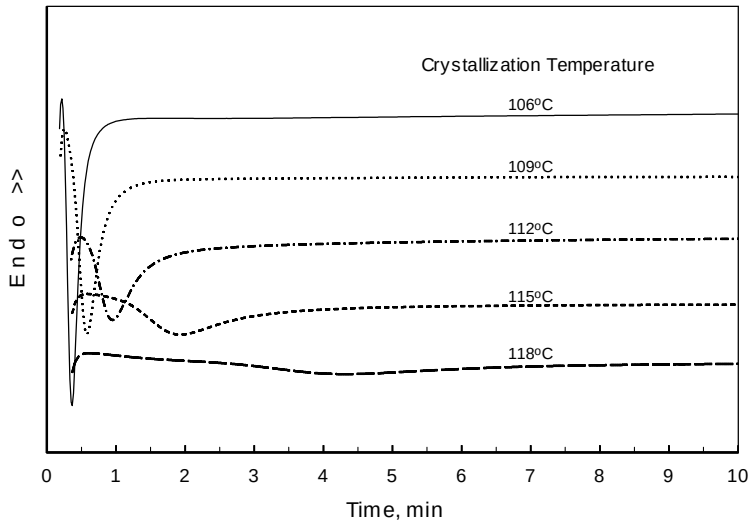

Fig. 11. DSC exothermic traces for P3DT isothermal crystallization at different temperatures.

seems in our case that the crystallinity has been well developed within 30 min. In addition, the shape of the endothermic peak seems to be more symmetric in our study, while P3DT showed a shoulder before the main melting process in the previous investigations [19].

The "down and up" phenomenon of melting peak temperatures is observed again when P3DT is crystallized at 115°C as shown in Fig. 16. When the sample is crystallized at 115°C for 1 min, only one small peak is found at 139.5°C. A small peak at ~143°C, corresponding to Peak 2 in Fig. 2, is developed when P3DT is crystallized for 1.5 min, and it appears as a shoulder when the crystallization time is prolonged. When the crystallization time is longer than 3 min, another peak at higher temperature, ~150.5°C, corresponding to Peak 3 in Fig. 2, is observed. It is worthy to note that this melting peak is developed when the crystallization time is longer than 3 min, which corresponds to the $t_{1/2}$ at that crystallization temperature. Further decreasing the crystallization temperature to 108°C leads to more clearer melting behavior as shown in Fig. 17. Up to three transitions can be easily discerned. As the $t_{1/2}$ at 108°C is very short, ~0.5 min, Peak 1 generally increases with time, while Peaks 2 and 3 are almost independent of crystallization time at this crystallization temperature.

Our experimental results do not support the existence of liquid crystalline phase in regioregular P3DT as the melting peaks at higher temperatures (Peaks 2 and 3) are formed with prolonged crystallization time or at lower crystallization temperature, T_c. Several reports have mentioned the existence of ordered, quasi-ordered and disordered phases in poly(3-alkylthiophene)s with high head–tail regularity. Our experiment clearly shows the development of three ordering processes during isothermal crystallization of

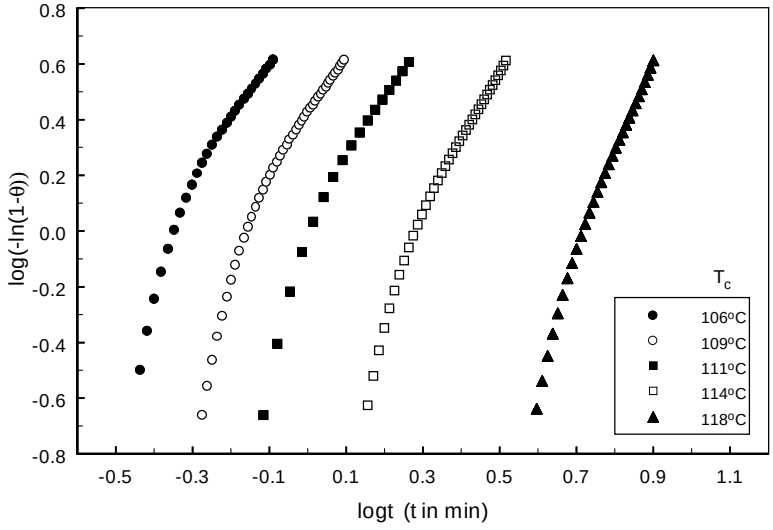

Fig. 12. Plot of $\log(-\ln(1-\theta))$ vs. $\log t$ for the isothermal crystallization of P3DT.

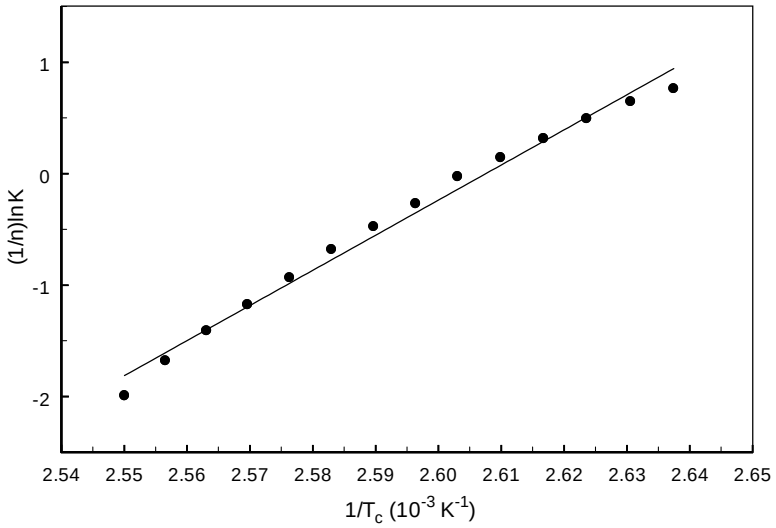

Fig. 13. Estimation of isothermal crystallization activation energy for P3DT.

P3DT which are dependent on crystallization temperature and time (Figs. 3, 4, 14–17). The plausible three ordered phases can be deducted from the isothermal crystallization and melting experiments: (A) quasi-ordered phase in which the thiophene rings exhibit to some degree twisting with respect to each other; (B) ordered phase in which the thiophene rings are well aligned and parallel to each other between layers; (C) ordered phase with zipper effect from the side chains, meaning that the side chains are oriented and take mainly *trans*-conformation. When the samples are non-isothermally crystallized by cooling from the isotropic melt, the crystallinity achieved is highly influenced by cooling rate. The low cooling rate leads to higher crystallinity due to the formation of large quantity of the quasi-ordered phase (Fig. 3). During isothermal crystallization at a fixed temperature, quasi-ordered phase (A) develops first from the isotropic melt. Later partial quasi-ordered phase will transform into the ordered phase (B). Owing to the higher thermal mobility of molecular chains at high crystallization temperature, the amount of this transformation is limited. During the transformation from the quasi-ordered phase to the ordered phase, the increased co-planarity of thiophene rings will enhance the interaction of the neighboring chains, the unit cell will shrink a little, thus the melting temperature of the quasi-ordered phase will decrease slightly. The lamellae thickening during long crystallization time will result in higher melting temperatures for the quasi-ordered phase. Park et al [19] reported two melting processes for the isothermally crystallized P3DT, which correspond to Peaks 1 and 2 in our study. We think the difference comes from the regularity of the samples. The P3DT sample used in our study has a regioregularity greater than 98.5%. Yang's experiments clearly showed that P3DT with 70% H–T regularity melted at 70°C, while P3DT with nearly

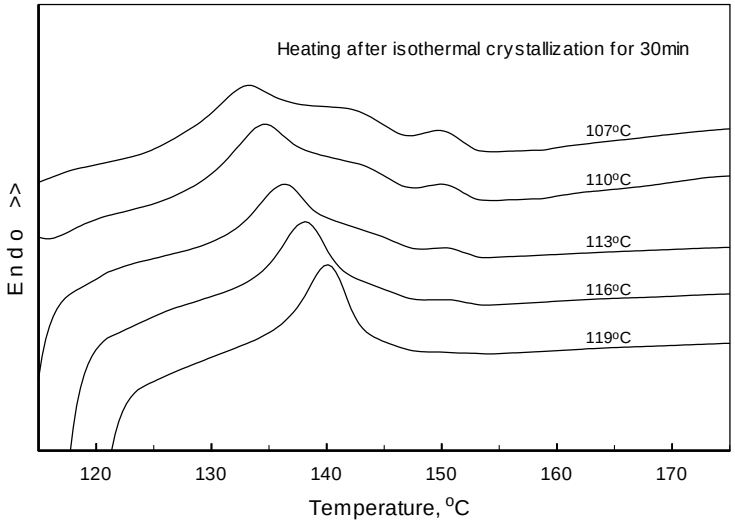

Fig. 14. Set of heating curves for P3DT crystallized for 30 min at different temperatures.

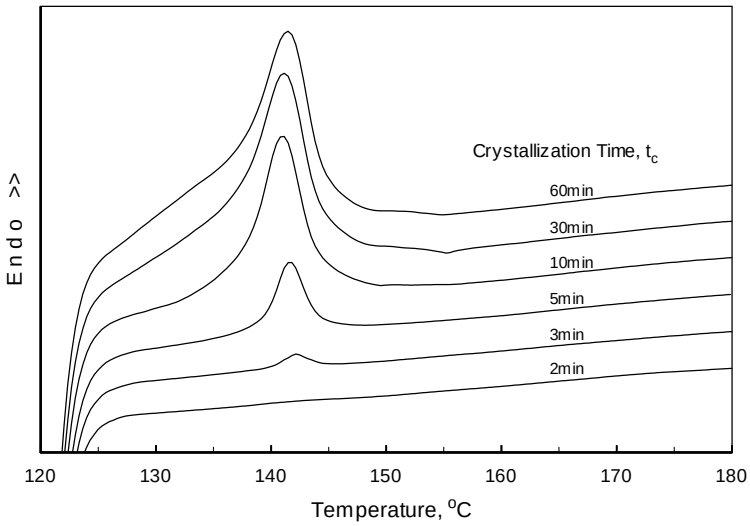

Fig. 15. DSC heating curves for P3DT crystallized at 120°C for different times.

100% H–T regularity exhibited two melting processes, one at low temperature and another at higher temperature [16].

As the side chains are in the molten state when the temperature is higher than 75°C as evidenced from Fig. 2, the zipper effect from the side chain seems to be questionable. However, spectroscopy studies revealed the conformational change from *gauche* to *trans* during cooling from the isotropic state [31]. The crystallization at 80°C and subsequent melting behavior would support the zipper effect from the side chain. The heating curves shown in Fig. 18 are independent of crystallization time for P3DT, while P3HT could continue to crystallize and form a low melting phase during annealing [32]. We consider that the side chains in P3DT will be oriented at relatively higher temperature so that they can form crystalline phase from the crystallized main chains when the temperature is decreased. Otherwise randomly oriented side chains cannot crystallize simultaneously.

4. Conclusions

The non-isothermal and isothermal crystallization and melting behavior of regioregular P3DT has been systematically studied with an emphasis on the main chain crystallization, ordering and melting. The Avrami analysis for the non-isothermal crystallization exhibited two linear regions with a transition when the relative crystallinity was about 63% for all the cooling rates studied. The Ozawa method failed to describe the non-isothermal crystallization process. The non-isothermal crystallization activation energy was obtained to be 222 kJ/mol by applying the Kissinger mothed, which exhibited good agreement with the estimated isothermal crystallization activation energy. The isothermal crystallization was performed at different temperatures. Three ordering processes were proposed according to the subsequent melting experiments: (1) formation of quasi-ordered phase; (2) ordered phase and (3) ordered phase

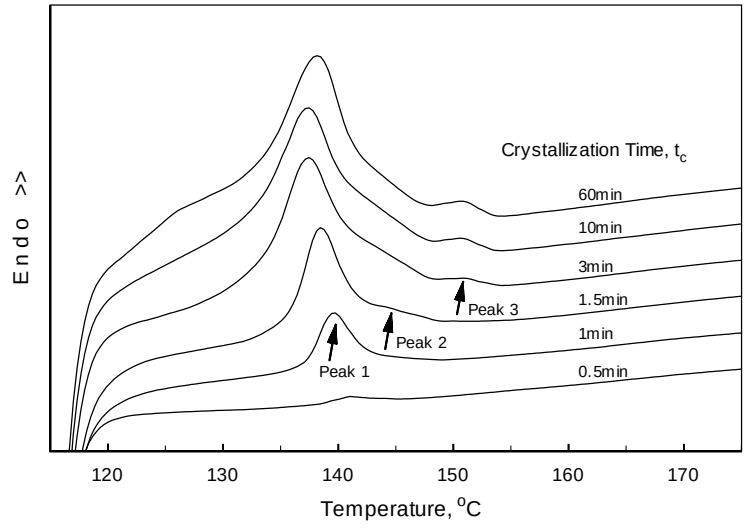

Fig. 16. DSC heating curves for P3DT crystallized at 115°C for different times.

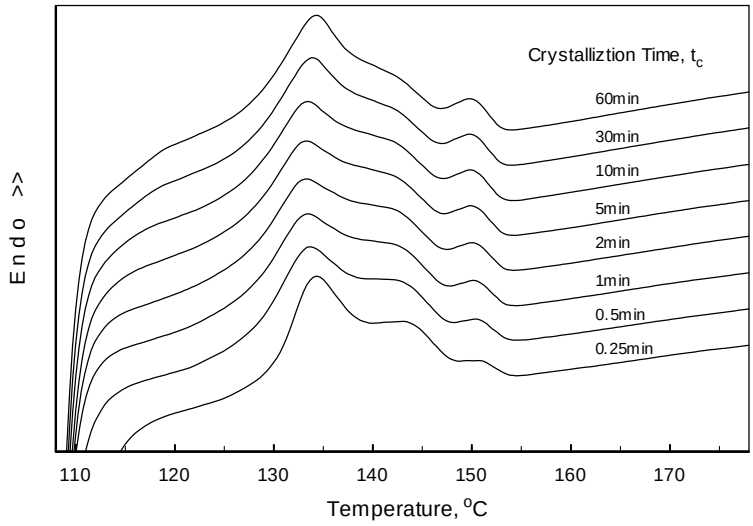

Fig. 17. DSC heating curves for P3DT crystallized at 108°C for different times.

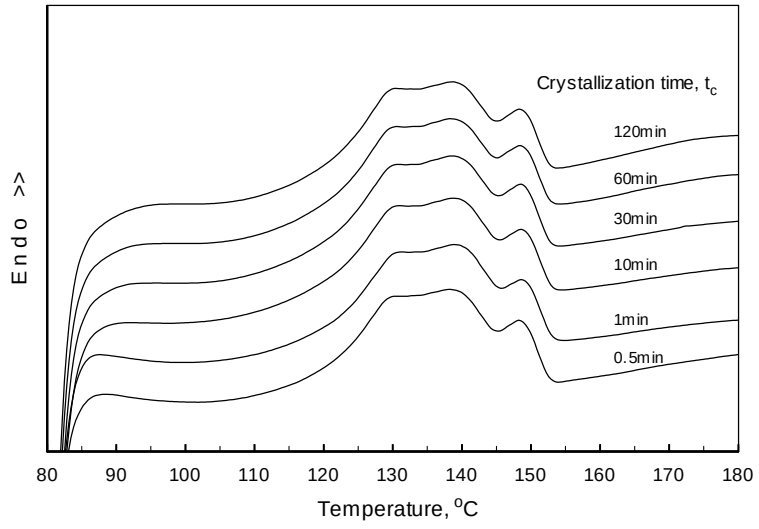

Fig. 18. DSC heating curves for P3DT crystallized at 80°C for different times.

with zipper effect from the side chains. The regioregularity and long chain character in the side chain of P3DT provide good opportunity to study the ordering processes in polymer crystallization. The zipper effect cannot be applied to those polymers without long side chains. As the three ordering processes during isothermal crystallization of P3DT were proposed based on DSC experiments, it should be examined by other experiments such as X-ray diffraction, FTIR and small angle X-ray scattering (SAXS).

Acknowledgements

The authors would like to thank Dr K.P. Pramoda for her useful discussions.

References

[1] Przyluski J. Conducting polymer—electrochemistry, Sci-Tech, 1991.
[2] Zheng WY, Levon K, Laakso J, Osterholm JE. Characterization and solid state properties of processable *N*-alkylated polyanilines in the neutral state. Macromolecules 1994;27:7754.
[3] Pei Q, Jarviene H, Osterholm JE, Inganas O, Laakso J. Poly[3-(4-octylphenyl)thiophene], a new processable conducting polymer. Macromolecules 1992;25:4297.
[4] McCullough RD, Lowe RD, Jayaraman M, Anderson DL. Design, synthesis, and control of conducting polymer architectures: structurally homogeneous poly(3-alkylthiophenes). J Org Chem 1993;58:904.
[5] Yamamoto T, Hayashi H. π-conjugated soluble and fluorescent poly-(thiophene-2,5-dily)s with phenolic, hindered phenolic and p-$C_6H_4OCH_3$ substitutes. Preparation, optical properties, and redox reaction. J Poly Sci, Part A: Polym Chem 1997;35:463.
[6] Bolognesi A, Catellani M, Destri S, Porzio W. Evidence of chain planarity in polyalkylthiophene: low-temperature structural analysis

of poly(3-decylthiophene). Makromol Chem, Rapid Commun 1991;12:9.
[7] Bolognesi A, Porzio W, Provasoli F, Ezquerra T. The thermal behavior of low-molecular-weight poly(3-decylthiophene). Makromol Chem 1993;194:817.
[8] Tashiro K, Kobayashi M, Kawai T, Yoshino K. Crystal structural change in poly(3-alkyl thiophene)s induced by iodine doping as studied by organized combination of X-ray diffraction, infrared/Raman spectroscopy and computer simulation techniques. Polymer 1997;38:2867.
[9] Schopf G, KoBmehl G. Polythiophenes: electrically conductive polymers, Berlin: Springer, 1997.
[10] Chen SA, Ni JM. Structure/properties of conjugated conductive polymers. 1. Neutral poly(3-alkylthiophene)s. Macromolecules 1992;25:6081.
[11] Yue S, Berry GC, McCullough RD. Intermolecular association and superamolecular organization in dilute solution. 1. Regioregular poly(3-dodecylthiophene). Macromolecules 1996;29:933.
[12] Tashiro K, Ono K, Minagawa Y, Kobayashi M, Kawai T, Yoshino K. Structure and thermochromic solid-state phase transition of poly-(3-alkylthiophene). J Polym Sci Polym Phys 1991;29:1223.
[13] Chen SA, Lee SJ. Application of molecular dynamics in determination of conformation change with temperature of poly(3-dodecylthiophene) in crystalline cell. Synth Met 1995;72:253.
[14] Prosa TJ, Winokur MJ, Moulton J, Smith P, Heeger AJ. X-ray structural studies of poly(3-alkylthiophenes): an example of an inverse comb. Macromolecules 1992;25:4364.
[15] Gallazzi MC, Castellani L, Zerbi G, Sozzani P. Synth Met 1991;41–43:495.
[16] Yang C, Orfine FP, Holdcroft S. A phenomenological model for predicting thermochromism of regioregular and nonregioregular poly(3-alkyithiophenes). Macromolecules 1996;29:6510.
[17] Park KC, Levon K. Order–disorder transition in the electroactive polymer poly(3-dodecylthiophene). Macromolecules 1997;30:3175.
[18] Kawai T, Nakazono M, Sugimoto R, Yoshino K. Change in crystal structure of poly(3-alkylthiophene) upon doping. Synth Met 1993;55–57:353.
[19] Rim PB, Runt JP. Melting behavior of crystalline/compatible polymer blends: poly(ϵ-carprolactone)/poly(styrene-co-acrylonitrile). Macromolecules 1983;16:762.
[20] Avrami M. Kinetics of phase change. I. General theory. J Chem Phys 1939;7:1103.
[21] Avrami M. Kinetics of phase change. II. Transformation–time relation for random distribution of nuclei. J Chem Phys 1940;8:212.
[22] Liu TX, Yu YM, Cui Y, Zhang HF, Mo ZS. Isothermal and nonisothermal crystallization kinetics of Nylon-11. J Appl Polym Sci 1998;70:2371.
[23] Liu TX, Mo ZS, Wang S, Zhang HF. Nonisothermal melt and cold crystallization kinetics of poly(aryl ether ether ketone ketone). Polym Engng Sci 1997;37:568.
[24] Ozawa T. A modified method for kinetic analysis of thermoanalytical data. J Therm Anal 1976;9:369.
[25] Cebe P, Hong SD. Crystallization behavior of poly(ether-ether-ketone). Polymer 1986;27:1183.
[26] Martins JCA, Novack KM, Gomes AS. Nonisothermal crystallization kinetics of thermotropic polyesters with flexible spacers in the main chain. Polymer 1998;39:6941.
[27] Srinivas S, Babu JR, Riffle JS, Wilkes GL. Kinetics of isothermal and nonisothermal crystallization of novel poly(arylene ether ether sulfide)s. Polym Engng Sci 1997;37:497.
[28] Liu TX, Mo ZS, Zhang HF. Nonisothermal crystallization behavior of a novel poly(aryl ether ketone): PEDEKmK. J Appl Polym Sci 1998;67:815.
[29] Kissinger HE. Reaction kinetics in differential thermal analysis. Anal Chem 1957;29:1703.
[30] Qian RY, Chen SX, Song WH, Bi XP. Evidence for the liquid-crystalline state of poly(3-hexylthiophene) melt. Macromol Rapid Commun 1994;15:1.
[31] Nakazono M, Kawai T, Yoshino K. Effects of heat treatment on properties of poly(3-alkylthiophene). Chem Mater 1994;6:864.
[32] Zhao YG, Roche YP. A calorimetric study of the phase transition in poly(3-hexylthiophene). Polymer 1995;36:2211.